INFLUENCE OF MATRIX ON THE CORROSION RESISTANCE OF ALUMINA-CHROMIA BRICKS FOR ROTARY TYPE WASTE MELTING FURNACES

Hitoshi Chiba, Hitoshi Toda, Shun Kawaguchi, Makoto Ohno, and Fumihito Ozeki
MINO CERAMIC CO.,LTD., Nagoya, Japan

ABSTRACT

Waste melting furnaces play a vital role in Japan because they make it possible to incinerate and melt industrial and household wastes at high temperatures, contributing to solution of landfill shortage problems and establishment of resource recycling society. Various types of waste melting furnaces have been developed depending on the kind of waste disposal process. Since refractory lining is exposed to intensive corrosive conditions at high temperatures, Al_2O_3-Cr_2O_3 refractories are typically applied in waste melting furnaces [1][2][3]. In this study, we investigated the relationship between chromia content in the matrix of Al_2O_3-Cr_2O_3 brick and the corrosion behavior.

INTRODUCTION

Waste melting furnaces are classified depending on the type of waste and disposal process and the properties required for the refractory lining vary according to the furnaces. For Al_2O_3-Cr_2O_3 brick used in rotary kiln type (RK-type) waste melting furnaces, it is necessary to have both corrosion resistance to molten slag and spalling resistance to mechanical stress during rotation and thermal shock.

In general, the higher the content of chromia in Al_2O_3-Cr_2O_3 brick, the weaker the spalling resistance. In order to achieve a long lifetime of the brick in actual kilns, it needs to contain a smaller amount of chromia but have high corrosion resistance.

POSTMORTEM ANALYSIS

The properties of Al_2O_3-Cr_2O_3 brick described in these postmortem analyses are shown in Table 1.

The microscopy image of boundary surface of Al_2O_3-Cr_2O_3 brick used in a RK-type waste melting furnace is shown in Figure 1 and its EDS mapping image is shown in Figure 2. The brick was in service for a year. The hot face of the brick was smooth due to the corrosion reaction with molten slag. Densified layer with high content of Fe was observed at the boundary between the brick and slag. The densified layer, in other words, the reacted layer was likely to decompose in the closer area to the slag. Additionally, preferential corrosion of alumina grains was observed in some areas. Under the boundary (brick side), No Fe constituent was detected while Ca and Si constituents are detected in the matrix, leading to the brick microstructure deterioration.

Tab. 1: Typical properties of Al_2O_3-Cr_2O_3 brick

Physical properties	
Apparent porosity / %	18.2
Bulk density / g･cm^{-3}	3.34
Cold crushing strength / MPa	108
Chemical compositions / mass%	
Al_2O_3	67
Cr_2O_3	20

The following tendency was observed in the area under Fe-rich conditions. (1) Increase of wear, (2) Preferential corrosion of alumina grains, (3) Existence of reacted layer with high content of Fe at the boundary, (4) Gradual deterioration of the matrix caused by Ca and Si constituents.

Taking into consideration the factors mentioned above, increasing wear of Al_2O_3-Cr_2O_3 brick is supposed to be caused by preferential corrosion of alumina grains. Therefore effective

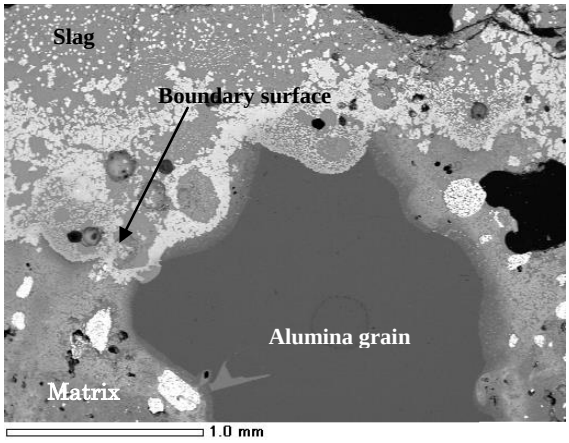

Fig. 1: Microscopy image of boundary surface of Al_2O_3-Cr_2O_3 brick used in a RK-type waste melting furnace

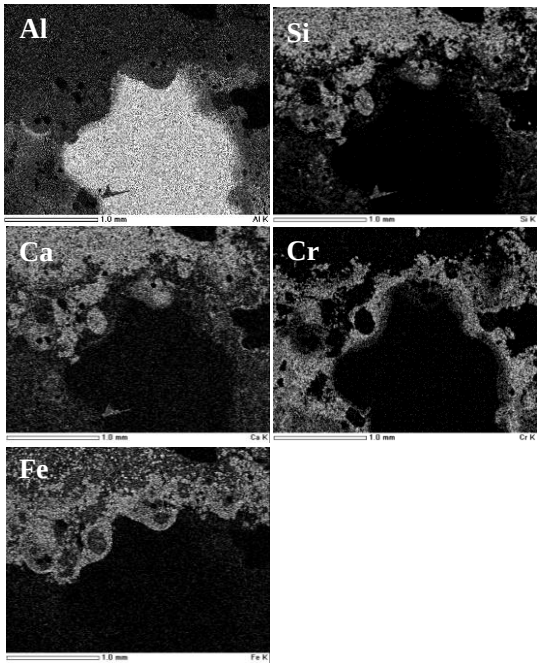

Fig. 2: EDS mapping image of Al, Si, Ca, Cr, Fe elements for Figure 1

Tab. 2: Composition of Al_2O_3-Cr_2O_3 samples used in the experiment

Specimens of AC20 series	AC20-0	AC20-5	AC20-10	AC20-20	AC20-30
Cr_2O_3 content of used grains / mass%	0	5	10	20	30
Cr_2O_3 content in matrix / mass%	18.1	16.0	13.8	9.7	5.5
Total content of Cr_2O_3 / mass%	20				
Specimens of AC30 series	AC30-0	AC30-5	AC30-10	AC30-20	AC30-30
Cr_2O_3 content of used grains / mass%	0	5	10	20	30
Cr_2O_3 content in matrix / mass%	21.9	20.0	18.1	14.1	10.1
Total content of Cr_2O_3 / mass%	30				

use of Al_2O_3-Cr_2O_3 solid solution grains and/or in-situ Al_2O_3-Cr_2O_3 solid solution will probably contribute to the improvement of the corrosion resistance of the Al_2O_3-Cr_2O_3 brick.

EXPERIMENTAL PROCEDURE

Influence of Fe element in the slag on alumina grains in the Al_2O_3-Cr_2O_3 bricks was evaluated.

Under the condition that the total chromia content is constant we prepared several specimens that have different chromia content in the grains and in the matrix. Fused Al_2O_3-Cr_2O_3 raw materials with 5, 10, 15, 20 and 30 mass% chromia content were used as grains. The composition of Al_2O_3-Cr_2O_3 brick samples containing 20 mass% and 30 mass% in total is shown in Table 2. AC20-0 represents the total chromia is 20 mass% and the grains chromia content is 0 mass%.

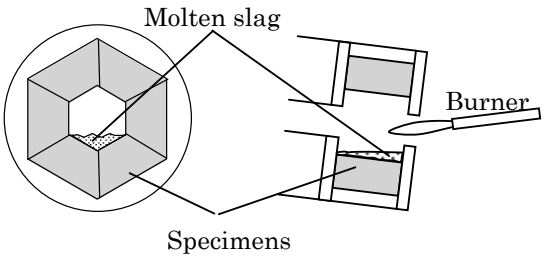

Fig. 3: Schema of rotary durum corrosion test apparatus

・Rotary durum corrosion test

A rotary durum corrosion test was conducted to evaluate the peeling and corrosion resistance of Al_2O_3-Cr_2O_3 bricks. The schema of rotary durum corrosion test apparatus is illustrated in Figure 3. It was heated up to 1600^0C in 5.5hrs, held at this temperature for 30 minutes, and then slag was fed at a rate of 300 grams per hour for 55 hrs. The slag for this test was prepared by mixing some commercially available chemicals so that the slag basicity is 0.5. Additionally, carbon grains and Fe-C pellets are added by certain amounts. After feeding the slag for 55 hrs, the apparatus was cooled to room temperature. The corrosion caused by molten slag was evaluated by measuring the depth of corrosion at eleven points with a vernier caliper compared to the original thicknesses.

・Microstructure analysis

The specimens after the test were analyzed by using SEM and EDS.

RESULTS AND DISCUSSION

・Rotary durum corrosion test

Cross sections of AC20 series brick after the test are shown in Figure 4. A dashed line represented the original thickness of the specimen. The corrosion depth of each specimen was measured at eleven points and the measured depth was averaged. Corrosion resistance indexes are calculated based upon the corroded depth of AC20-0 brick, which was converted to 100. The corrosion resistance indexes of both bricks are shown in Figure 5. The corresponding data of cross sections and the indexes in case of AC30 series brick are shown in Figure 6 and Figure 7. Corrosion resistance indexes of AC30 series are calculated based upon the

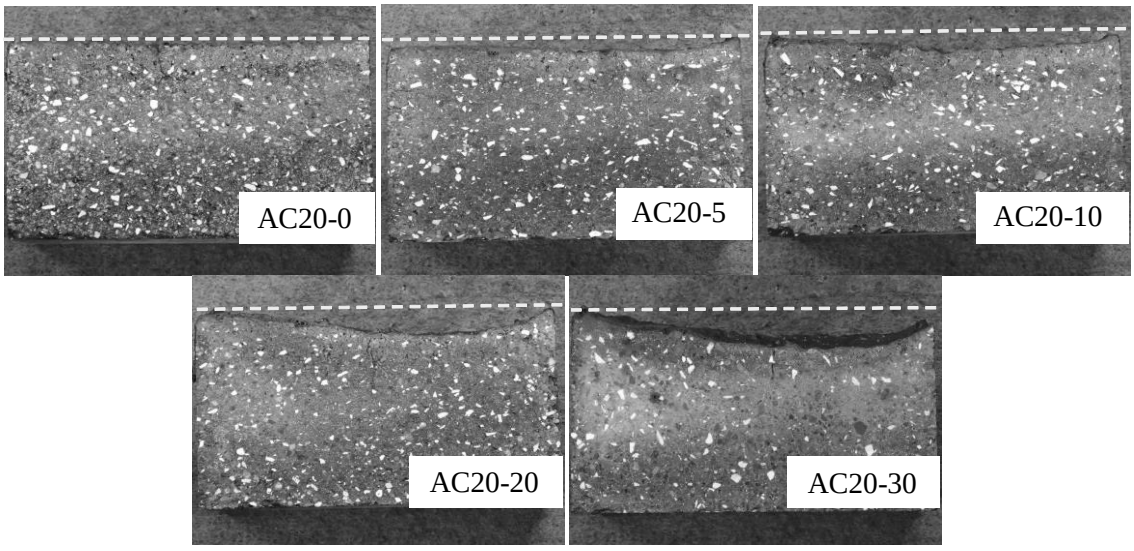

Fig. 4: Cross sections of AC20 series after the rotary durum corrosion test

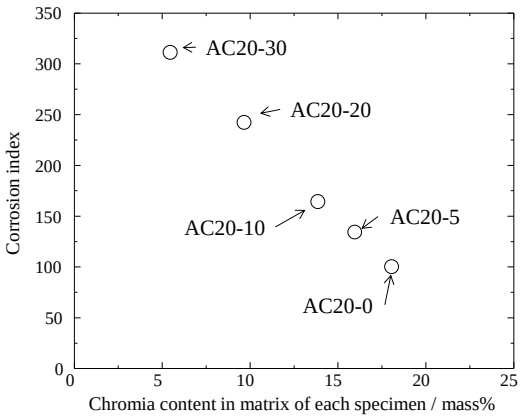

Fig. 5: Results of corrosion index of AC20 series

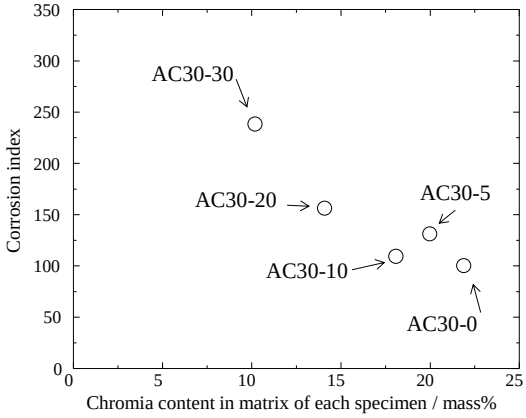

Fig. 7: Results of corrosion index of AC30 series

corroded depth of AC30-0 brick. The smaller index means the superior corrosion resistance. The results indicated the AC20-0 has the highest corrosion resistance of all AC20 series. Similarly AC30-0 has highest corrosion resistance of all AC30 series. It can be considered that the higher content of chromia in the matrix contributed to the higher corrosion resistance of Al_2O_3-Cr_2O_3 bricks.

・Microstructure analysis

Microscopy images of AC20-0 and AC20-30 after the test are shown in Figure 8 and Figure 9. Table 3 shows the chemical compositions measured at the spot (1), (2) and (3) in Figure 8 and Figure 9.

In AC20-0, the alumina grains were preferentially corroded and the reacted compounds with iron oxide, which seems to be hercynite ($FeAl_2O_4$), are formed into the slag. In AC20-30, on the other hand, the Al_2O_3-Cr_2O_3 grains protruded through the specimen surface, exhibiting slower corrosion of the grains.

A white belt formed by the reaction of the specimen with slag was observed in all specimens. The chemical compositions of the white belt are almost the same in both AC20-0 and AC20-30 even though the chromia content in the matrix is 12% or more different each other. According to the EDS analysis, the white belt is composed of the solid solution of hercynite ($FeAl_2O_4$) and chromite ($FeCr_2O_4$). The thickness of the reacted layer (white belt) was different depending on the spot and it was observed that the higher the chromia content in the matrix, the thicker the layer. As an example, the layer width was 510 μm in AC20-0 and 120 μm in AC20-30.

Enlarged microscopy image of the boundary surface of AC20-0 after the test is shown in Figure 10. Table 4 shows the chemical composition measured at the spot (4) and (5) in Figure 10. Although the slag composed of Ca and Si infiltrated deeper, almost no Fe constituent was seen in the infiltrated constituents. From the results, we believe that iron oxide in the slag reacted rapidly with Al_2O_3-Cr_2O_3 at the boundary surface and the reacted layer was formed.

The reacted layer was densified at the boundary but thinner at the side of slag and then decomposed into the slag. These results indicate that the specimen was corroded by the decomposition of the reacted layer into the slag.

As shown in AC20-0 and AC20-30, AC30-0 and AC30-30 displayed the white belt at the boundary surface between the specimen and slag, which is composed of solid solution of hercynite ($FeAl_2O_4$) and chromite ($FeCr_2O_4$). Additionally, preferential corrosion of alumina grains was observed in AC30-0. From the observation described above, AC30 series were corroded by the same mechanism as AC20 series.

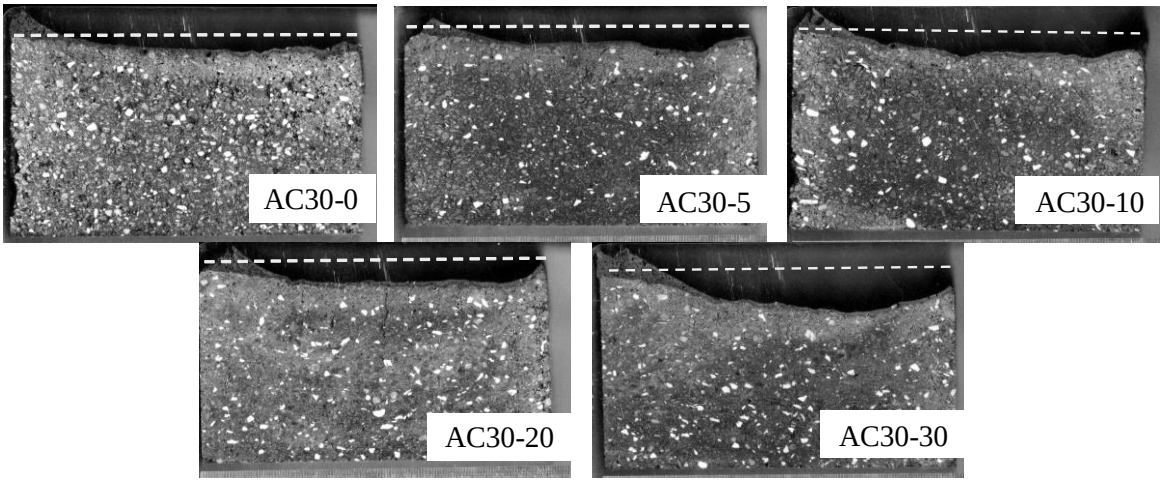

Fig. 6: Cross sections of AC30 series after the rotary durum corrosion test

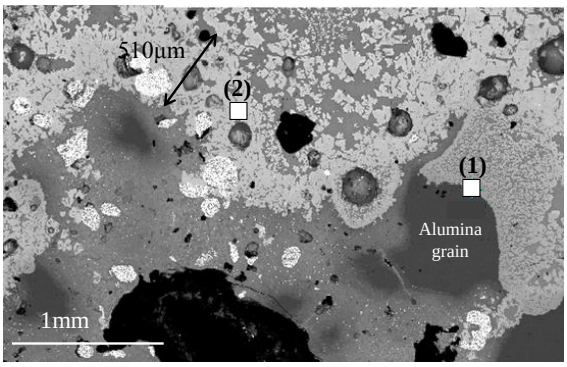

Fig. 8: Microscopy image of AC20-0 boundary surface between the specimen and slag after the test

Tab. 3: Chemical composition measured at the spot (1), (2) and (3) in Fig. 8 and Fig. 9

Chemical composition	(1)	(2)	(3)
Al_2O_3 / mass%	52.3	25.5	25.7
SiO_2 / mass%	0.9	0.8	0.8
CaO / mass%	0.1	0.1	0.1
Cr_2O_3 / mass%	0.6	32.9	35.0
Fe_2O_3 / mass%	46.3	40.6	38.1

Tab. 4: Chemical composition measured at the spot (4) and (5) in Fig. 10

Chemical composition	(4)	(5)
Al_2O_3 / mass%	31.2	28.0
SiO_2 / mass%	36.8	40.6
CaO / mass%	17.6	18.0
Cr_2O_3 / mass%	0.8	0.8
Fe_2O_3 / mass%	1.1	1.2

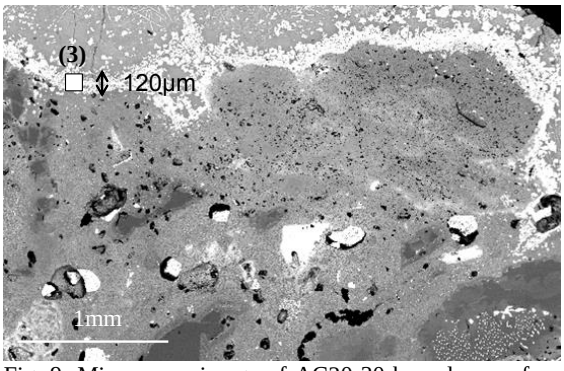

Fig. 9: Microscopy image of AC20-30 boundary surface between the specimen and slag after the test

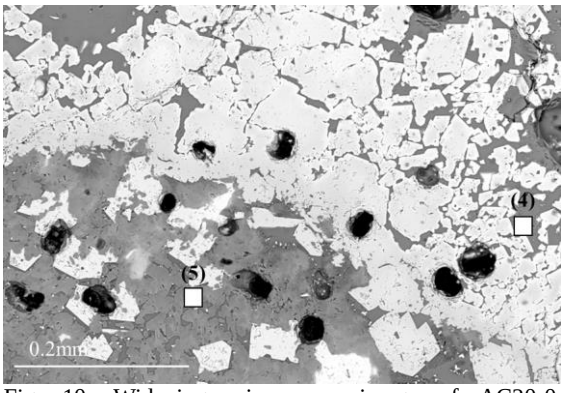

Fig. 10: Widening microscopy image of AC20-0 boundary surface between the specimen and slag after the test

CONCLUSIONS

Taking into consideration the factors mentioned above, the wear mechanism of Al_2O_3-Cr_2O_3 bricks is considered as follows.

(1) Molten slag penetrates refractories.
(2) Iron oxide in the infiltrated constituents reacts with refractories and the reacted layer composed of solid solution of hercynite ($FeAl_2O_4$) and chromite ($FeCr_2O_4$) is formed.
(3) The reacted layer gradually decomposed into slag.

The results demonstrated the higher content of chromia in the matrix contributed to the higher corrosion resistance of Al_2O_3-Cr_2O_3 bricks.

The Al_2O_3-Cr_2O_3 bricks of AC20-0 and AC30-0 showed superior performance in a RK-type waste melting furnaces. The other factor of the superior performance is high spalling resistance to mechanical stress during rotation and thermal shock.

In order to meet the customers' demand, we will continue to improve the quality of our Al_2O_3-Cr_2O_3 bricks.

REFERENCES

[1] Hisanori Hoshizuki, Hiroyuki Tanida, Yasutaka Yoshimi and Satoshi Ota : Taikabutsu, 64[12] 582-583(2012).
[2] Hitoshi Chiba, Hisanori Hoshizuki, Hiroyuki Tanida and Yoshiki Tsuchiya : Taikabutsu, 65[12] 586-587(2013)
[3] Ryuuta Mitsui and Yasutaka Yoshimi : Taikabutsu, 67[12] 610-611(2015)